Desalination and Water Treatment
www.deswater.com

doi: 10.5004/dwt.2022.28443

259 (2022) 152–159
May

Co–Fe–B nanofilaments as high-performance catalysts for hydrogen generation from the hydrolysis of $NaBH_4$ solution

Honghui Chen[a], Xue Wang[b], Di Zhang[b], Yifan Wu[a], Ke Zhang[b], Zhongqiu Cao[b], Shiwei Wu[b], Kezhen Qi[b], Yan Wang[b,*], Guode Li[b,*], Peng Yu[a,*]

[a]*College of Chemistry and Materials Science, Hunan Agricultural University, Changsha, Hunan 410128, PR China, Tel. 86-731-84617022; emails: pengy7505@hunau.edu.cn (P. Yu), whu019@163.com (H. Chen), 504946983@qq.com (Y. Wu)*
[b]*Institute of Catalysis for Energy and Environment, College of Chemistry and Chemical Engineering, Shenyang Normal University, Shenyang 110034, PR China, Tel. 86-24-86576903; email: wangyan11287@mail.nankai.edu.cn (Y. Wang), Tel. 86-24-86593318; emails: 1052434792@qq.com (G. Li), 763077660@qq.com (X. Wang), 296783960@qq.com (D. Zhang), zhangke@synu.edu.cn (K. Zhang), caozhongqiu6508@sina.com (Z. Cao), wsw@synu.edu.cn (S. Wu), qkzh2003@aliyun.com (K. Qi)*

Received 16 November 2021; Accepted 27 March 2022

ABSTRACT

The strategy of hydrogen generation from sodium borohydride ($NaBH_4$) hydrolysis has obtained extensive attention in the past decade, but it is restrained by the high cost and limited abundance for the used noble metal catalysts. Herein, we prepare noble-metal-free Co–Fe–B catalysts on Cu sheet, which can reduce the cost to satisfy the demand of practical application. The as-synthesized high-performance Co–Fe–B catalysts show filamentous structure by optimizing pH value to 12.0, providing more contact areas and active sites on reaction interface. Compared with the binary Co–B and Fe–B materials, the ternary Co–Fe–B nanofilaments exhibit good catalytic performance for dehydrogenation from the $NaBH_4$ hydrolysis. The catalyzed hydrogen generation rate (HGR) of Co–Fe–B can achieve 9,408.9 mL min^{-1} g^{-1} at 25°C. The HGR value is 1.5 times higher than Co–B and 2.6 times higher than Fe–B under the same condition. Moreover, the result suggests that $NaBH_4$ hydrolysis process is independent of the amount of added catalysts, which means that it is a zero-order reaction. This work sheds light on the vital role of the cooperative action between different elements and the unique microstructure for designing high-performance catalysts.

Keywords: Sodium borohydride; Hydrogen generation kinetics; Cooperative action; Filamentous Co–Fe–B; hydrolysis

1. Introduction

In the past few decades, the development of efficient and clean energy replacement has been considered to be a hotspot to resolve a range of environmental issues such as the shortage of fossil energy and climate warming [1–4]. Sodium borohydride ($NaBH_4$) has caused more public concern owing to its high hydrogen density (10.6 wt.%), good solubility in water and non-toxicity [5–8]. The stored hydrogen can be released by the means of $NaBH_4$ hydrolysis with proper catalysts. For noble metal catalysts, they can possess good catalytic activity. However, the high cost and limited abundance unavoidably hinder the extensive application of hydrogen generation from $NaBH_4$ solution [9–11]. To date, noble-metal-free catalysts have received tremendous interests because of the bargain prices, rich reserves and enhanced activity. It contains Co-based, Ni-based, and Cu-based catalysts.

As early as 1971, the reaction mechanism of $NaBH_4$ hydrolysis has been reported by Holbrook and Twist [12].

* Corresponding authors.

The authors have revealed that $-BH_3$ in the cracked B–H bond firstly integrates with the active site (M) on the catalyst surface to form with the species $M–BH_3^-$. After that, OH^- attacks $M–BH_3^-$ to product intermediate BH_3 and transfer electrons to M (e_M). And then, e_M transfers to neighboring H_2O molecular and form M–H. Finally, M–H integrates with the other M–H species from BH_4^- to create a H_2 molecule. It can be inferred the surface structure of catalysts is an important factor for improving the catalytic performance. Therefore, various catalyst materials with different structures have been reported, such as, nanosheets [13] nanoflowers [14], nanoarrays [15], hollow structures [16], and nanoparticles [17], and so on. In addition, it has been pointed out that combining with different non-noble metals and metalloid is another effective method to increase the catalytic performance. Yang et al. [18] reported that the ternary Ni–Fe–P catalyst showed the outstanding catalytic performance when compared with binary Ni–P and Fe–P. Li et al. [19] pointed out that the activity of NiCoP nanosheet array outperformed most Co based catalysts and some precious metal based catalysts for $NaBH_4$ hydrolysis. It should be noted that nanoparticles prepared by the traditional liquid phase reduction are in a powdery form, which are difficult to separated and easily aggregated because of the high surface area. Compared with the traditional liquid phase reduction, electroless plating method is employed to prepare thin-film catalysts on numerous substrate materials. It can avoid above-mentioned problems and enhance the catalytic performance. Moreover, the thin-film catalysts easily recover and benefit the recycling test during the hydrolysis of $NaBH_4$.

Hence, in view of the above unique feature, we design Co–Fe–B catalyst system containing two non-noble metals and one metalloid with unique filamentous structure. The Co–Fe–B catalysts are prepared on Cu sheet by electroless plating method. It has been confirmed that Co–Fe–B is an economical and efficient catalyst toward the hydrogen generation from the hydrolysis of alkaline $NaBH_4$ solution. The obtained hydrogen generation rate is 1.5 times and 2.6 times higher than Co–B and Fe–B under the same conditions, respectively.

2. Experimental

2.1. Synthesis of Co–Fe–B catalysts

Co–Fe–B catalysts were synthesized by electroless plating method. Firstly, Cu sheet with an apparent surface area of 4 cm^2 × 4 cm^2 was successively handled with alkaline solution, acid solution, sensitizing solution and activate solution. And then, 1.1896 g $CoCl_2·6H_2O$, 1.1122 g $FeSO_4·7H_2O$, and 4.5042 g $C_2H_5NO_2$ were dissolved into 80 mL deionized water in a 200 mL beaker. Then, the solution pH value ranged from 11.0 to 12.5 was adjusted by the NaOH solution (4 g NaOH, 20 mL deionized water). The temperature was set at 25°C by the thermostatic water bath. After that, 6.8094 g $NaBH_4$ was added into the aforementioned solution. Finally, the pretreated Cu sheet was used as the substrate and carried out the deposition process for 5 min. A series of Co–Fe–B samples were synthesized on the Cu sheet by changing the deposition pH value. Moreover, binary Co–B and Fe–B samples were also prepared through the same method. In particular, the calculation of the hydrogen generation rate is in view of the weight of Co–Fe–B, Fe–B or Co–B without Cu sheet.

2.2. Samples characterization

X-ray diffraction (XRD, Rigaku-Dmax 2500, Cu Kα radiation) was used to analyze the phase composition of the as-synthesized catalysts. Scanning electron microscopy (SEM, Hitachi S-4800), transmission electron microscopy (TEM, JEOL JEM-2100) were employed to study the surface microstructure. Inductively coupled plasma-mass spectroscopy (ICP-MS, Agilent 7900) was adopted to observe the element composition. Brunauer–Emmett–Teller (BET) measurement was carried out by N_2 adsorption–desorption isotherms at 77 K (TriStar II 3020).

2.3. Hydrolytic dehydrogenation of $NaBH_4$

0.1 g NaOH was dissolved into 10 mL distilled water in a 20 mL two-necked flask. Then, 0.5 g $NaBH_4$ was added slowly into the alkaline solution. After it is entirely dissolved, a certain amount of Co–Fe–B (Co–B or Fe–B) catalyst was rapidly placed into the flask in a thermostatic water bath. The released hydrogen was collected by the water displacement method. The hydrolytic dehydrogenation reaction was performed at 25°C, 30°C, 35°C, and 40°C to determine the apparent activation energy (E_a). The hydrogen generation rate is abbreviated to hydrogen generation rate (HGR), which is a crucial parameter that is used to evaluate the catalytic activity towards the hydrolysis of $NaBH_4$. The HGR value can be obtained by fitting the slope of a plot of H_2 evolution volume vs. time in the linear range. It can be expressed by the following equation:

$$\mathrm{HGR} = \frac{V_{\mathrm{H_2}}}{m_{\mathrm{catalyst}} \cdot t} \tag{1}$$

where the parameters of V_{H_2}, $m_{catalyst}$ and t are the volume number of the generated H_2^2, the total weight of the catalyst used, and the corresponding hydrolysis reaction time, respectively. The unit of HGR can be expressed as mL min^{-1} g^{-1} or L min^{-1} g^{-1}.

3. Results and discussion

Fig. 1 displays the XRD patterns of the Co–Fe–B samples deposited at pH ranged from 11.0 to 12.5. It can be observed that their phase compositions have no notable difference. Except for the diffraction peak of the substrate Cu (JCPDS No. 70-3038) at 2θ = 43.2°, 50.3°, and 73.9°, Fe_3B (JCPDS No. 39-1316) and Co (JCPDS No. 1-1255) can be clearly seen. In addition, some weak diffraction peaks can be attributed to the Co_3O_4 phase (JCPDS No. 80-1537). The reason may be the contact between the Co–Fe–B samples and atmospheric oxygen during the material synthesis or stockpile as previously reported [20]. Table 1 lists the composition of Co, Fe, and B element. The result displays that atomic ratio of Co, Fe, and B is 1:1.03:0.76,

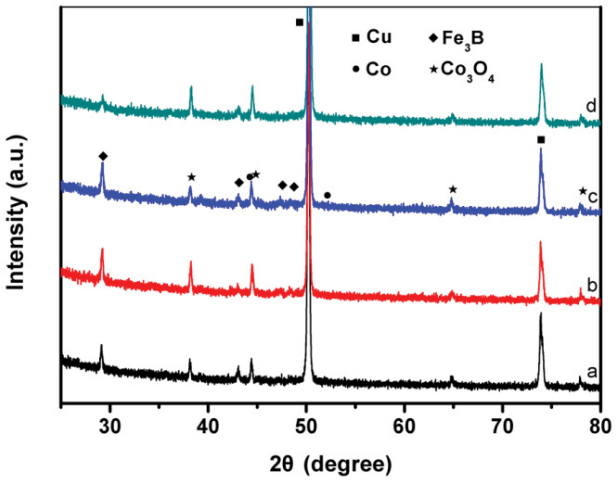

Fig. 1. XRD patterns of the Co–Fe–B samples at different pH values: (a) pH = 11.0, (b) pH = 11.5, (c) pH = 12.0 and (d) pH = 12.5, respectively.

1:0.95:0.69, 1:0.77:0.63, and 1:0.72:0.63 when the solution pH value is 11.0, 11.5, 12.0 and 12.5, respectively. Therefore, the corresponding Co–Fe–B samples can be labeled as $CoFe_{1.03}B_{0.76}$, $CoFe_{0.95}B_{0.69}$, $CoFe_{0.77}B_{0.63}$, and $CoFe_{0.72}B_{0.63}$. It can be inferred that pH value has remarkably affected the chemical composition of the as-prepared Co–Fe–B samples.

In order to observe the surface microstructure of the as-obtained Co–Fe–B samples at different pH values, the SEM images are exhibited in Fig. 2. It can be seen that Co–Fe–B samples prepared at pH = 11.0 and 11.5 are composed of irregular spheres (Fig. 2a and b). When the pH value was increased to 12.0, SEM image (Fig. 2c) reveals that there are some hollow structures on the surface of the irregular spheres, which is more obvious based on the amplifying SEM image (Fig. 2e). With further raising the pH value to 12.5, the synthesized Co–Fe–B is still irregular spheres, but the number of the hollow structures becomes less from the SEM image in Fig. 2d. TEM technique has been employed for the Co–Fe–B irregular spheres to figure out the detailed structural information. As shown in Fig. 2f and g of different magnification, it can be seen that Co–Fe–B irregular sphere consists of filamentous structure. Its diameter and length is approximately 6.0–8.5 nm and 30–50 nm, respectively. The hollows can also be obviously found from TEM image in Fig. 2g, which is consistent with the findings of SEM image as shown in Fig. 2e. In addition, BET specific surface area is calculated to be 21.2 $m^2 g^{-1}$, along with the adsorption average pore diameter is about 10.30 nm, respectively.

To research the effect of the solution pH value on the catalytic performance, the hydrolysis experiment was performed at pH = 11.0, 11.5, 12.0, and 12.5, respectively. Fig. 3a displays the catalytic activity of the as-obtained different Co–Fe–B samples toward the hydrogen generation from the $NaBH_4$ hydrolysis. It can be found that different Co–Fe–B samples show variant catalytic activity. Apparently, Co–Fe–B catalyst deposited at pH = 12.0 shows the good catalytic performance with the fast HGR value of 9,408.9 mL $min^{-1} g^{-1}$ at 25°C (Fig. 3b). The good catalytic activity may be attributed to the unique filamentous structure which is conducive to the increase of the specific surface area, resulting in the enhancement of transmission of generated hydrogen from $NaBH_4$ solution on the catalyst surface as previously reported by Jadhav et al. [21]. In addition, to compare with the catalytic performance of binary and ternary catalysts, the kinetics curve of $NaBH_4$ hydrolysis by adding Co–B, Fe–B, and Co–Fe–B catalysts (pH = 12.0) was provided in Fig. 3c. Based on corresponding HGR histogram as shown in Fig. 3d, the result displays that the obtained HGR of Co–Fe–B catalyst is 9,408.9 mL $min^{-1} g^{-1}$ at 25°C, which is 1.5 and 2.6 times higher than Co–B and Fe–B under the same condition, respectively. It can be inferred that the synergistic effect of different element is especially important for improving the catalytic activity as reported by Patel et al. [22].

It is well known that the hydrolysis solution of $NaBH_4$ is alkaline to prevent from itself hydrolysis. Hence, it is necessary to discuss the effect of the concentration of NaOH on the hydrogen generation kinetics. Fig. 4a exhibits the kinetics curve of different $NaBH_4$ solution catalyzed by the Co–Fe–B catalyst (pH = 12.0). NaOH concentration is 1, 3, 5, 7, 10, 15, and 20 wt.%, respectively. According to the line chart in Fig. 4b, it can be seen that the HGR value increases from 9,408.9 to 9,614.2 mL $min^{-1} g^{-1}$ with changing NaOH concentration from 1 to 3 wt.%, and then gradually reduces to 3,018.8 mL $min^{-1} g^{-1}$ when NaOH concentration increases to 20 wt.%. Therefore, it can be concluded that the optimal NaOH concentration is 3 wt.% for $NaBH_4$ hydrolysis catalyzed by the as-obtained Co–Fe–B catalyst. This similar phenomenon has been stated for Co–B/Activated carbon and Co–Ni–B catalyst by previously reported [23,24]. It well known that the hydrolysis solution contains two kinds of anions, OH^- and BH_4^-. They dated from an excessive amount of NaOH solution and $NaBH_4$ solution, respectively. The transfer of anions to the catalytic surface is the key for the process

Table 1
ICP-MS analysis of element composition of the Co–Fe–B samples at different pH values

ICP-MS results	pH value			
	11.0	11.5	12.0	12.5
Co (at.%)	35.82	37.88	41.78	42.66
Fe (at.%)	37.02	35.82	32.10	30.59
B (at.%)	27.16	26.30	26.12	26.75
Co:Fe:B (at.%)	1:1.03:0.76	1:0.95:0.69	1:0.77:0.63	1:0.72:0.63

of hydrogen generation [25]. To a certain extent, if redundant OH^- anions occupy the catalyst surface, the hydrogen generation rate will lower because of the decrease of BH_4^- anions which is used to produce hydrogen. Hence, the NaOH concentration needs to be controlled to an optimal value which is not only employed to maintain the alkaline hydrolysis solution, but also prevents its diffusion to the catalyst surface.

In order to ascertain the influence of catalyst amount on the HGR, the hydrolysis tests of $NaBH_4$ solution were carried out by applying various amounts of the Co–Fe–B catalyst (pH = 12.0), including 1.85, 3.8, 6.8, and 9.7 mg. The corresponding hydrogen generation kinetics curve is given in Fig. 5a, the HGR values are 8,952.4; 9,098.56; 9,408.9 and 9,141.9 mL min^{-1} g^{-1}, respectively. Fig. 5b provides the plot of the HGR vs. the catalyst amounts both in natural logarithmic scales to calculate the reaction order. The result displays that the fitted slope is 0.02, which is approximately zero, illustrating the zero-order reaction on account of Co–Fe–B amount.

The apparent activation energy (E_a) is a significant parameter for discussing the catalytic hydrolysis of $NaBH_4$ solution. In view of this, we choose four various temperatures to observe the hydrogen generation kinetics. Fig. 6a reveals the time plots of the dehydrogenation kinetics by using the Co–Fe–B catalysts (pH = 12.0) at 25°C, 30°C, 35°C, and 40°C, respectively. As was expected, the HGR is incremental with the increase of the hydrolysis temperature from 25°C to 40°C. Based on the state equation of ideal gas, the HGR constant (k, mol min^{-1} g^{-1}) can be reckoned at different temperatures. The corresponding Arrhenius plots (ln$k$ vs. 1/T) obtained from the kinetic data can be shown

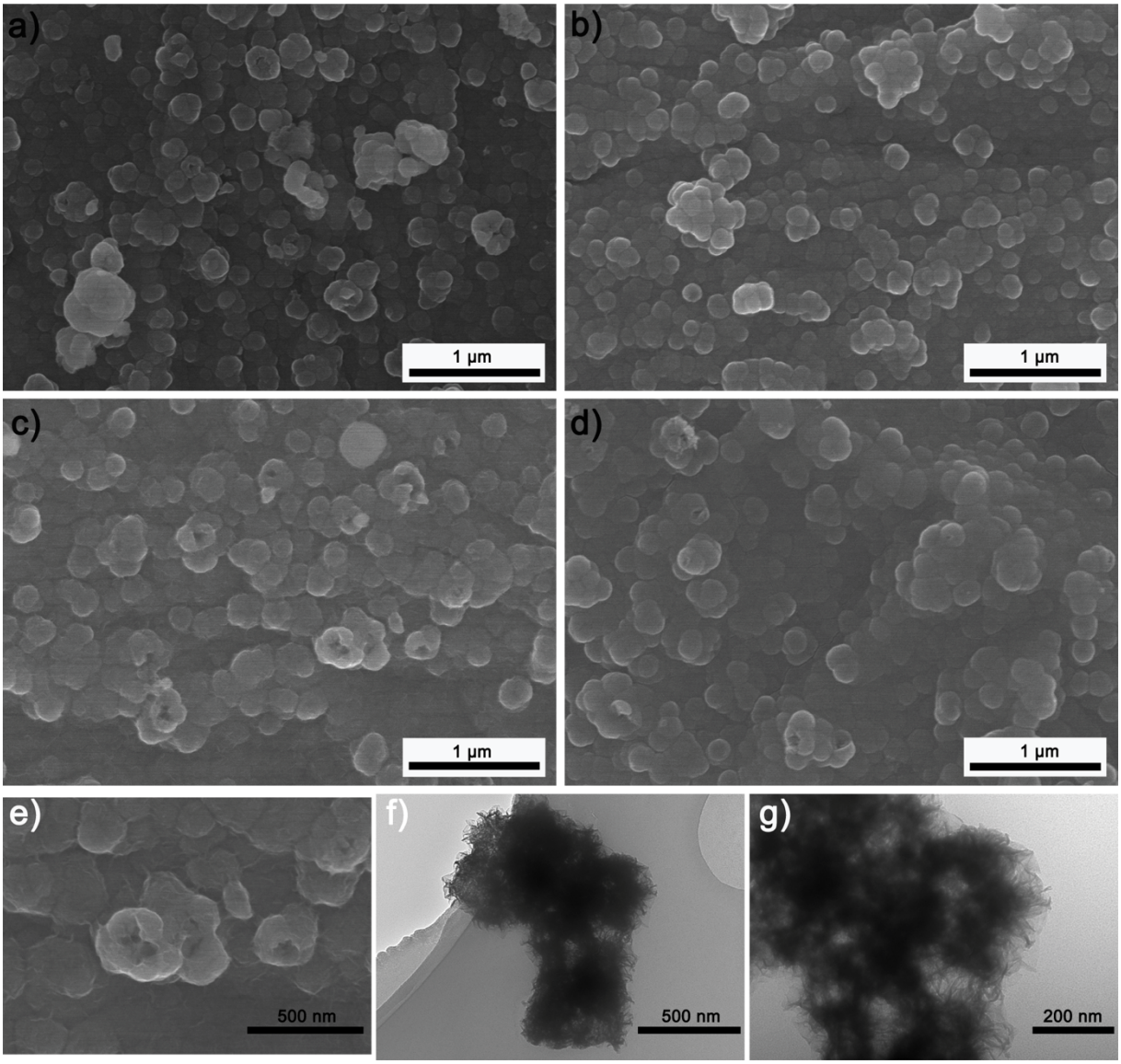

Fig. 2. SEM images of the Co–Fe–B samples at various pH values: (a) pH = 11.0, (b) pH = 11.5, (c, e) pH = 12.0, (d) pH = 12.5; (f, g) TEM images of the as-obtained Co–Fe–B catalyst (pH = 12.0).

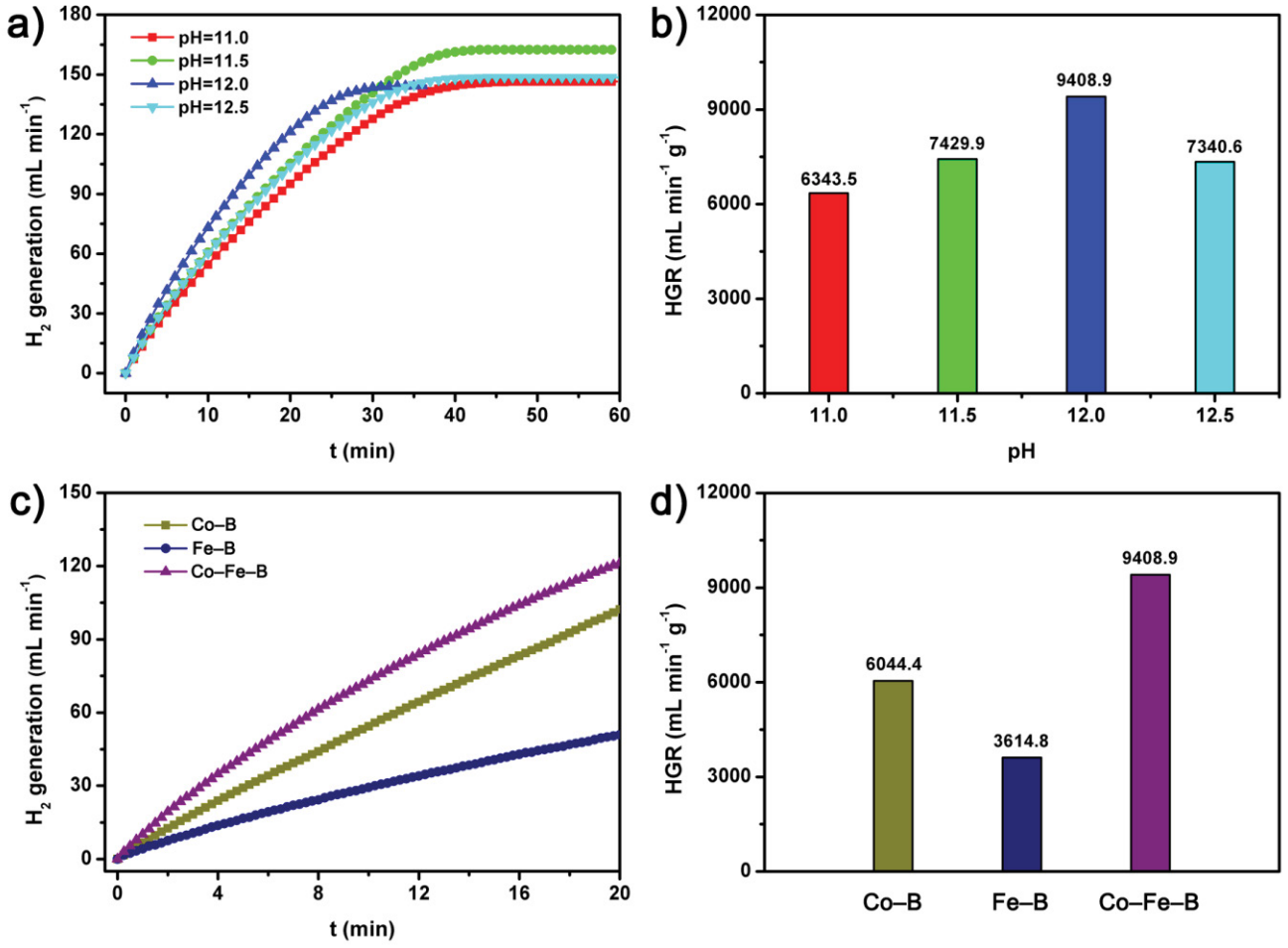

Fig. 3. (a) Hydrogen generation kinetics curve, and (b) the corresponding HGR histogram of the $NaBH_4$ hydrolysis catalyzed by different Co–Fe–B samples at pH = 11.0, 11.5, 12.0, and 12.5; (c) Hydrogen generation kinetics curve and (d) the corresponding HGR histogram of the $NaBH_4$ hydrolysis catalyzed by Co–B, Fe–B, and Co–Fe–B catalysts.

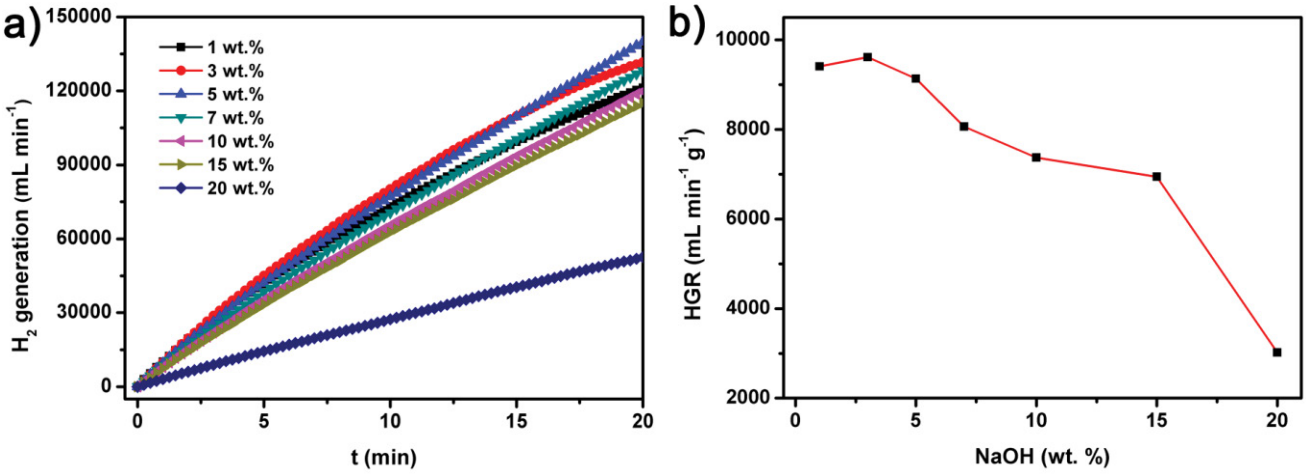

Fig. 4. (a) The hydrogen generation kinetics curve and (b) the corresponding HGR histogram of the $NaBH_4$ hydrolysis catalyzed by Co–Fe–B catalysts (pH = 12.0) at different NaOH concentrations.

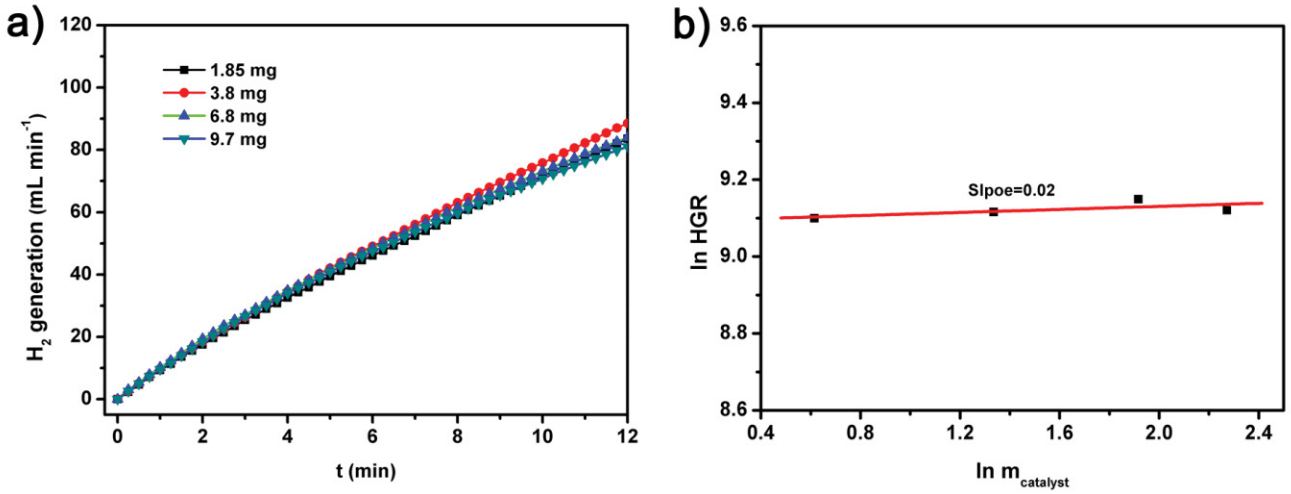

Fig. 5. (a) Time plots of the dehydrogenation from $NaBH_4$ hydrolysis catalyzed by various amounts of the Co–Fe–B catalyst (pH = 12.0) and (b) plot of the HGR vs. the catalyst amounts both in natural logarithmic scale.

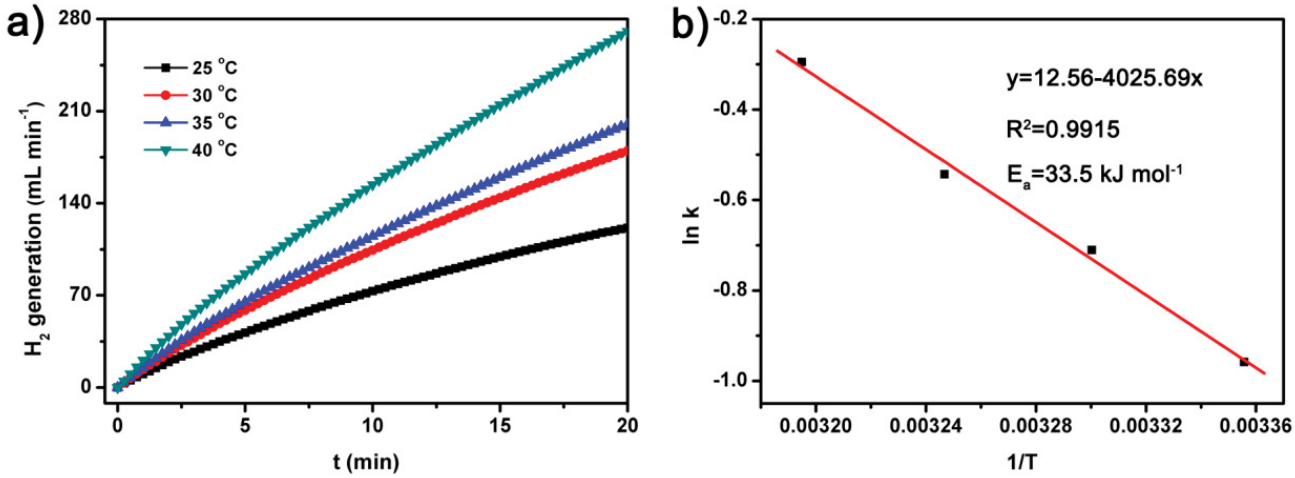

Fig. 6. (a) The curve of hydrogen generation kinetics for $NaBH_4$ hydrolysis catalyzed by Co–Fe–B catalysts (pH = 12.0) at different temperature and (b) the corresponding Arrhenius plots (ln$k$ vs. 1/T).

in Fig. 6b. E_a value is calculated to be 33.5 kJ mol^{-1} on the basis of the Arrhenius equation. An intuitive comparison about the HGR and E_a has been given in Fig. 7 according to the previous reports. Fig. 7 has been divided into four regions when it was centered in the red point (HGR, E_a) of this work. By contrast, it can be found that E_a value in this work is lower than that of most listed catalysts in Region 1 and 2 in the literature, including Co–Cr–B/CeO_2 [26], p(HEMA)/Co [27], Co–Ni–P/Cu sheet [28], Fe–CoP/Ti [15], Co–B [29], Co–B hollow spheres [30], Co–P [14,17,31], Co–Cu–B [32], Ru–IRA-400 [33], Co–Ni–P/Pd–TiO_2 [34], Co–B/Carbon [35], CoO nanocrystals [36], Co–P/Cu sheet [37], Co–B [38], Ru–SZ [39], CSAC–supported Co–Ce–B [40], except for Co–B-10CNTs [41], Co–P/Cu sheet [42], Co/γ–Al_2O_3 [43], and Co–B/Ni foam [44] in Region 3 and 4. For the HGR, it is clear that the as-obtained HGR for the Co–Fe–B is only lower than that of Co–B-10CNTs [41] and CSAC-supported Co–Ce–B [40], but higher than that of the all of catalysts located in Region 1and 2. It is well known that it should show high HGR and low E_a for an efficient catalyst. Hence, the as-prepared Co–Fe–B catalyst in this work will possess potential application prospect to some extent.

4. Conclusions

In summary, noble-metal-free Co–Fe–B has been prepared on Cu sheet and employed as the efficient catalyst for the hydrolysis of $NaBH_4$ solution. The composition, microstructure and catalytic activity are greatly influenced by the solution pH value. The optimum ternary Co–Fe–B catalyst shows much higher catalytic performance than that of the binary Co–B and Fe–B materials. The high HGR of Co–Fe–B can achieve 9,408.9 mL min^{-1} g^{-1} at 25°C, which

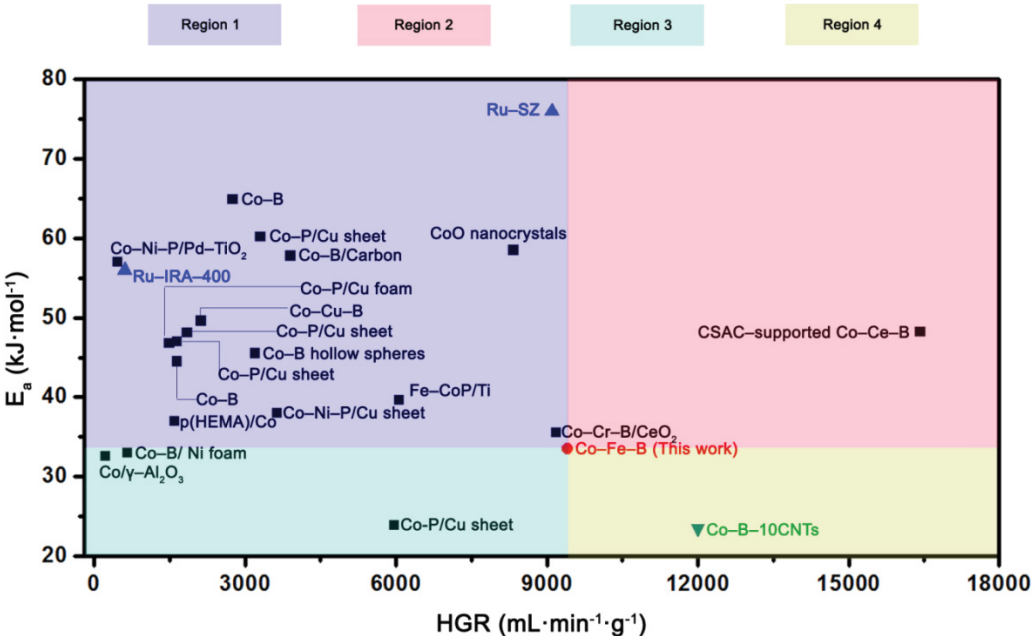

Fig. 7. The scatter diagrams of HGR vs. E_a of the reported metal-based materials for the hydrolysis of $NaBH_4$ solution.

should attribute to the cooperative action between different elements and the unique microstructure. In addition, the kinetics has been investigated based on the amount of added catalysts, the result presents that the hydrolysis process is a zero-order reaction.

Notes

The authors declare no competing financial interest.

Acknowledgments

This work was supported by the National Natural Science Foundation of China (22075186, 21975164), the Scientific Research Fund of Liaoning Provincial Education Department (LJKZ0997, LJKZ0993), the Revitalization Talents Program (XLYC1907013) of Liaoning Province, Liaoning BaiQianWan Talents Program, the Science and Technology Project of Shenyang (21-108-9-05), the Hundred Talent Program (SSDBRJH1902002) and Major Incubation Project (ZD202003) of Shenyang Normal University.

References

[1] J. Guo, B. Wang, D. Yang, Z. Wan, P. Yan, J. Tian, T.T. Isimjan, X. Yang, Rugae-like Ni_2P-CoP nanoarrays as a bi-functional catalyst for hydrogen generation: $NaBH_4$ hydrolysis and water reduction, Appl. Catal., B, 265 (2020) 118584, doi: 10.1016/j.apcatb.2019.118584.

[2] H. Zhang, Y. Li, W. Li, C. Zhuang, C. Gao, W. Jiang, W. Sun, K. Qi, Z. Sun, X. Han, Designing large-sized cocatalysts for fast charge separation towards highly efficient visible-light-driven hydrogen evolution, Int. J. Hydrogen Energy, 46 (2021) 28545–28553.

[3] Y. Wang, Z. Hu, W. Chen, S. Wu, G. Li, S. Chou, Non-noble metal-based catalysts applied to hydrogen evolution from hydrolysis of boron hydrides, Small Struct., 2 (2021) 2000135, doi: 10.1002/sstr.202000135.

[4] M.N. Raache, M.H. Sellami, M.R. Kouadri, A. Benarima, Photocatalysts behavior during hydrogen generation by water electrolysis under solar rays, Desal. Water Treat., 212 (2021) 428–433.

[5] H.I. Schlesinger, H.C. Brown, A.E. Finholt, J.R. Gilbreath, H.R. Hoekstra, E.K. Hyde, Sodium borohydride, its hydrolysis and its use as a reducing agent and in the generation of hydrogen, J. Am. Chem. Soc., 75 (1953) 215–219.

[6] X. Zhang, Y. Cheng, C. Li, Q. Guo, X. Meng, Catalytic hydrolysis of alkaline sodium borohydride solution for hydrogen evolution in a micro-scale fluidized bed reactor, Int. J. Energy Res., 44 (2020) 6758–6766.

[7] H.N. Abdelhamid, A review on hydrogen generation from the hydrolysis of sodium borohydride, Int. J. Hydrogen Energy, 46 (2021) 726–765.

[8] N. Gilani, J.V. Pasikhani, P.T. Motie, M. Akbari, Fabrication of quantum Cu(II) nanodot decorated TiO_2 nanotubes by the photochemical deposition-assisted hydrothermal method: study catalytic activity in hydrogen generation, Desal. Water Treat., 139 (2019) 145–155.

[9] A. Zabielaitė, A. Balčiūnaitė, I. Stalnionienė, S. Lichušina, D. Šimkūnaitė, J. Vaičiūnienė, B. Šimkūnaitė-Stanynienė, A. Selskis, L. Tamašauskaitė-Tamašiūnaitė, E. Norkus, Fiber-shaped Co modified with Au and Pt crystallites for enhanced hydrogen generation from sodium borohydride, Int. J. Hydrogen Energy, 43 (2018) 23310–23318.

[10] Y. Bai, C. Wu, F. Wu, B. Yi, Carbon-supported platinum catalysts for on-site hydrogen generation from $NaBH_4$ solution, Mater. Lett., 60 (2006) 2236–2239.

[11] S.C. Amendola, S.L. Sharp-Goldman, M.S. Janjua, M.T. Kelly, P.J. Petillo, M. Binder, An ultrasafe hydrogen generator: aqueous, alkaline borohydride solutions and Ru catalyst, J. Power Sources, 85 (2000) 186–189.

[12] K.A. Holbrook, P.J. Twist, Hydrolysis of the borohydride ion catalysed by metal–boron alloys, J. Chem. Soc., A, (1971) 890–894.

[13] L. Gong, K. Lan, X. Wang, X. Huang, P. Jiang, K. Wang, M. Yang, L. Ma, R. Li, Carbon-coated Co-Mo-P nanosheets supported on carbon cloth as efficient electrocatalyst for hydrogen evolution reaction, Int. J. Hydrogen Energy, 45 (2020) 544–552.

[14] Y. Wang, K.Z. Qi, S.W. Wu, Z.Q. Cao, K. Zhang, Y.S. Lu, H.X. Liu, Preparation, characterization and catalytic sodium

borohydride hydrolysis of nanostructured cobalt-phosphorous catalysts, J. Power Sources, 284 (2015) 130–137.
[15] C. Tang, R. Zhang, W. Lu, L. He, X. Jiang, A.M. Asiri, X. Sun, Fe-doped CoP nanoarray: a monolithic multifunctional catalyst for highly efficient hydrogen generation, Adv. Mater., 29 (2016) 1–6, doi: 10.1002/adma.201602441.
[16] H.Z. Guo, X. Liu, Y.H. Hou, Q.S. Xie, L.S. Wang, H. Geng, D.L. Peng, Magnetically separable and recyclable urchin-like Co–P hollow nanocomposites for catalytic hydrogen generation, J. Power Sources, 260 (2014) 100–108.
[17] T.H. Oh, S. Kwon, Effect of manufacturing conditions on properties of electroless deposited Co–P/Ni foam catalyst for hydrolysis of sodium borohydride solution, Int. J. Hydrogen Energy, 37 (2012) 15925–15937.
[18] J.G. Yang, Q. Yuan, Y. Liu, X.L. Huang, Y.X. Qiao, J.N. Lu, C.L. Song, Low-cost ternary Ni-Fe-P catalysts supported on Ni foam for hydrolysis of ammonia borane, Inorg. Chem. Front., 6 (2019) 1189–1194.
[19] K. Li, M. Ma, L. Xie, Y. Yao, R. Kong, G. Du, A.M. Asiri, X. Sun, Monolithically integrated NiCoP nanosheet array on Ti mesh: an efficient and reusable catalyst in $NaBH_4$ alkaline media toward on-demand hydrogen generation, Int. J. Hydrogen Energy, 42 (2017) 19028–19034.
[20] D. Ke, Y. Tao, Y. Li, X. Zhao, L. Zhang, J. Wang, S. Han, Kinetics study on hydrolytic dehydrogenation of alkaline sodium borohydride catalyzed by Mo-modified Co-B nanoparticles, Int. J. Hydrogen Energy, 40 (2015) 7308–7317.
[21] A.R. Jadhav, H.A. Bandal, H. Kim, $NiCo_2O_4$ hollow sphere as an efficient catalyst for hydrogen generation by $NaBH_4$ hydrolysis, Mater. Lett., 198 (2017) 50–53.
[22] N. Patel, R. Fernandes, A. Miotello, Hydrogen generation by hydrolysis of $NaBH_4$ with efficient Co–P–B catalyst: a kinetic study, J. Power Sources, 188 (2009) 411–420.
[23] D. Xu, P. Dai, Q. Guo, X. Yue, Improved hydrogen generation from alkaline $NaBH_4$ solution using cobalt catalysts supported on modified activated carbon, Int. J. Hydrogen Energy, 33 (2008) 7371–7377.
[24] D. Xu, H. Wang, Q. Guo, S. Ji, Catalytic behavior of carbon supported Ni–B, Co–B and Co–Ni–B in hydrogen generation by hydrolysis of KBH_4, Fuel Process. Technol., 92 (2011) 1606–1610.
[25] C.-H. Liu, B.-H. Chen, C.-L. Hsueh, J.-R. Ku, F. Tsau, K.-J. Hwang, Preparation of magnetic cobalt-based catalyst for hydrogen generation from alkaline $NaBH_4$ solution, Appl. Catal., B, 91 (2009) 368–379.
[26] M.S. İzgi, O. Baytar, Ö. Şahin, H.Ç. Kazıcı, CeO_2 supported multimetallic nano materials as an efficient catalyst for hydrogen generation from the hydrolysis of $NaBH_4$, Int. J. Hydrogen Energy, 45 (2020) 34857–34866.
[27] F. Seven, N. Sahiner, Superporous P(2-hydroxyethyl methacrylate) cryogel-M (M:Co, Ni, Cu) composites as highly effective catalysts in H_2 generation from hydrolysis of $NaBH_4$ and NH_3BH_3, Int. J. Hydrogen Energy, 39 (2014) 15455–15463.
[28] Y. Guo, Q. Feng, J. Ma, The hydrogen generation from alkaline $NaBH_4$ solution by using electroplated amorphous Co–Ni–P film catalysts, Appl. Surf. Sci., 273 (2013) 253–256.
[29] P. Krishnan, S.G. Advani, A.K. Prasad, Thin-film CoB catalyst templates for the hydrolysis of $NaBH_4$ solution for hydrogen generation, Appl. Catal., B, 86 (2009) 137–144.
[30] H. Ma, W. Ji, J. Zhao, J. Liang, J. Chen, Preparation, characterization and catalytic $NaBH_4$ hydrolysis of Co-B hollow spheres, J. Alloys Compd., 474 (2009) 584–589.
[31] X. Zhang, J. Zhao, F. Cheng, J. Liang, Z. Tao, J. Chen, Electroless-deposited Co–P catalysts for hydrogen generation from alkaline $NaBH_4$ solution, Int. J. Hydrogen Energy, 35 (2010) 8363–8369.
[32] X.-L. Ding, X. Yuan, C. Jia, Z.-F. Ma, Hydrogen generation from catalytic hydrolysis of sodium borohydride solution using Cobalt–Copper–Boride (Co–Cu–B) catalysts, Int. J. Hydrogen Energy, 35 (2010) 11077–11084.
[33] S.C. Amendola, S.L. Sharp-Goldman, M.S. Janjua, N.C. Spencer, M.T. Kelly, P.J. Petillo, M. Binder, A safe, portable, hydrogen gas generator using aqueous borohydride solution and Ru catalyst, Int. J. Hydrogen Energy, 25 (2000) 969–975.
[34] M. Rakap, E.E. Kalu, S. Özkar, Cobalt–nickel–phosphorus supported on Pd-activated TiO_2 (Co–Ni–P/Pd-TiO_2) as cost-effective and reusable catalyst for hydrogen generation from hydrolysis of alkaline sodium borohydride solution, J. Alloys Compd., 509 (2011) 7016–7021.
[35] J. Zhao, H. Ma, J. Chen, Improved hydrogen generation from alkaline $NaBH_4$ solution using carbon-supported Co–B as catalysts, Int. J. Hydrogen Energy, 32 (2007) 4711–4716.
[36] A. Lu, Y. Chen, J. Jin, G.-H. Yue, D.-L. Peng, CoO nanocrystals as a highly active catalyst for the generation of hydrogen from hydrolysis of sodium borohydride, J. Power Sources, 220 (2012) 391–398.
[37] K. Eom, K. Cho, H. Kwon, Effects of electroless deposition conditions on microstructures of cobalt–phosphorous catalysts and their hydrogen generation properties in alkaline sodium borohydride solution, J. Power Sources, 180 (2008) 484–490.
[38] S.U. Jeong, R.K. Kim, E.A. Cho, H.J. Kim, S.W. Nam, I.H. Oh, S.A. Hong, S.H. Kim, A study on hydrogen generation from $NaBH_4$ solution using the high-performance Co–B catalyst, J. Power Sources, 144 (2005) 129–134.
[39] U.B. Demirci, F. Garin, Kinetics of Ru-promoted sulphated zirconia catalysed hydrogen generation by hydrolysis of sodium tetrahydroborate, J. Mol. Catal. A: Chem., 279 (2008) 57–62.
[40] X. Zhang, C. Li, J. Qu, Q. Guo, K. Huang, Cotton stalk activated carbon-supported Co–Ce–B nanoparticles as efficient catalysts for hydrogen generation through hydrolysis of sodium borohydride, Carbon Resour. Convers., 2 (2019) 225–232.
[41] L. Shi, Z. Chen, Z. Jian, F. Guo, C. Gao, Carbon nanotubes-promoted Co–B catalysts for rapid hydrogen generation via $NaBH_4$ hydrolysis, Int. J. Hydrogen Energy, 44 (2019) 19868–19877.
[42] Y.P. Guo, Q.H. Feng, Z.P. Dong, J.T. Ma, Electrodeposited amorphous Co-P catalyst for hydrogen generation from hydrolysis of alkaline sodium borohydride solution, J. Mol. Catal. A: Chem., 378 (2013) 273–278.
[43] W. Ye, H. Zhang, D. Xu, L. Ma, B. Yi, Hydrogen generation utilizing alkaline sodium borohydride solution and supported cobalt catalyst, J. Power Sources, 164 (2007) 544–548.
[44] H.-B. Dai, Y. Liang, P. Wang, H.-M. Cheng, Amorphous cobalt–boron/nickel foam as an effective catalyst for hydrogen generation from alkaline sodium borohydride solution, J. Power Sources, 177 (2008) 17–23.